2026 IEEE/SICE International Symposium on System Integration (SII)
January 11-14, 2026. Cancún, México

Single-chamber Inflatable Robot Arm with a Four-finger Gripper Driven by Built-in Pouch Muscles

Masayuki Otsuka[1] and Ryuma Niiyama[1]

***Abstract*— Inflatable robots are a class of soft robots that are suitable for human robot interaction, but their control complexity and safety remain challenging. We propose a soft inflatable robot in which the exterior, continuously supplied with air by a blower, serves as the skin, and a pouch muscle embedded within the skin and actuated by air pressure serves as the muscle. This system, termed the "musculo-skin system," forms the basis for developing an inflatable robotic arm with six degrees of freedom, including the shoulder, elbow, and four-finger gripper. The angles of the shoulder and elbow joints were measured and the angles and motion speeds of the joints were evaluated using data from the time series of each joint. To evaluate the fingers, a Rock-Paper-Scissors gesture was performed, demonstrating the ability to execute complex finger movements without interference. The experimental results confirmed that the finger movements were smooth and capable of performing natural gestures. These results will contribute to enabling more complex motions in soft inflatable robots.**

I. INTRODUCTION

Inflatable robots offer advantages such as lightweight structure, safety, space efficiency, and ease of scaling up. They are well-suited for human interaction [1] [2] [3].When focusing on the actuation system of inflatable robots, they can be classified into two types: Extrinsic actuators, where the driving source, for example a motor, is concentrated at the base and driven via wires, and Intrinsic actuators, such as pneumatic actuators, where actuators are placed between links and drive the robot's movement.

Each type has its own advantages and disadvantages. For extrinsic actuators [4] [5], one advantage is that concentrating the driving source outside the structure allows the robot to be lighter and more compact. However, as the number of joints increases, issues such as wire slack and complex routing arise, making control and maintenance more difficult. Therefore, this type of actuator is not suitable for highly articulated robots, such as those used for fingers. As shown in Fig. 1, a robotic arm with a total of six degrees of freedom, including the shoulder, elbow, and four fingers, was fabricated. Using this robotic arm, the range of motion and motion speed of the shoulder and elbow joints were measured. In addition, focusing on the four-finger gripper, hand gestures and object grasping tasks were performed.

For intrinsic actuators [6] [7] [8] [9], it is common to place actuators between links and drive the links through pneumatic expansion. They offer the advantage of easy modularization, making them suitable for robots that need to be scaled up or have a large number of joints. Additionally, since the actuators are integrated into the links, they contribute to space-saving. However, a disadvantage is that the overall structure becomes larger. Nevertheless, one of the characteristics of inflatable robots is that, unlike rigid robots whose mass increases proportionally to volume when scaled, the mass of inflatable robots increases proportionally to surface area. This characteristic allows inflatable robots to remain lightweight even when the structure is enlarged compared to rigid robots, thereby mitigating the disadvantage of size scaling associated with intrinsic actuators.

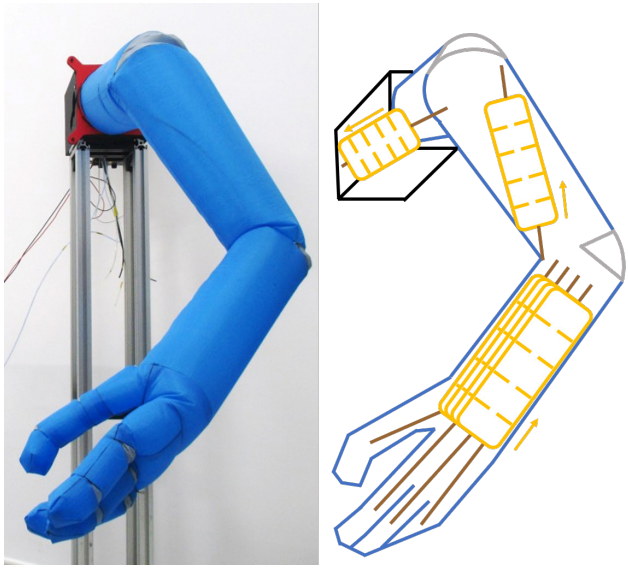

Fig. 1. Inflatable robotic arm

In research on inflatable robots with intrinsic actuators, a common approach is to place the actuators between links and generate motion through their inflation. This method requires the links to have a certain level of rigidity and is typically used in combination with links that are fully inflated and completely sealed, called closed inflatable links. However, in this configuration, the actuators are exposed to the outside, which raises safety concerns. Furthermore, the closed inflatable structure closes upon inflation, making it difficult to house the actuators inside. However, by combining the system with a structure that is air is continuously supplied from a blower, called an opened inflatable structure. The inflatable structure is maintained in an open state, ensuring that the actuators are housed inside and protected from external contact. This design offers the advantage of improved safety.

In this study, we propose a robotic arm that incorporates pouch muscles as intrinsic actuators within an inflatable

[1]Graduate School of Science and Technology, Meiji University, 1-1-1 Higashimita, Tama-ku, Kawasaki-shi, Kanagawa,Japan

robot. For this purpose, we adopted the pouch motor proposed by Niiyama et al. [10]. The pouch muscle is fabricated from a thin film material that, like the inflatable robot itself, forms a balloon-like structure. It is created by heat-sealing two sheets of film to form a sealed bag structure. Owing to its extremely thin profile, it is highly compact and can be freely arranged inside the inflatable body. In addition, it demonstrates high compatibility with inflatable structures as a pneumatic actuator. The use of film material enables the actuator to be both flexible and lightweight, facilitating internal integration while also contributing to low manufacturing cost. The actuators were installed inside an open inflatable robot that is continuously supplied with air from a blower. By embedding the actuators internally, the link diameter remains unchanged, and the actuators are completely enclosed without external exposure. The outer surface of the inflatable structure functions as an element analogous to human skin. We refer to this integrated structure of an open inflatable shell and internal actuators as the musculo-skin system. One of the advantages of the musculo-skin system is its high flexibility and contact safety, which make it suitable for robots that interact with humans. Therefore, as shown in Fig. 1, a 6-degree-of-freedom robotic arm was developed, consisting of shoulder and elbow joints that mimic human joint structures, as well as a four-finger gripper. To evaluate the effectiveness of the musculo-skin system, the range of motion and bending speed of the shoulder and elbow joints were measured. Furthermore, focusing on the four-finger gripper, hand gesture motions and object-grasping tasks were conducted. The main contribution of this study lies in the proposal of a novel musculo-skin system, which combines an intrinsic actuator with an opened inflatable structure, thereby significantly contributing to the field by demonstrating the effectiveness of a new driving method for inflatable robots.

II. METHOD

A. Principle of Operation

The target inflatable joint is constructed as shown in Fig. 2. It is based on the soft inflatable joints proposed by Seong et al. [11] and Niiyama et al. [4] . The cylindrical fabric structure inflates by continuously supplying air from a blower. Inside the robotic arm, pouch muscles are installed as actuators. The attachment points of the pouch muscles are located on the side opposite to the leaf-shaped patch of the target joint. Each pouch muscle extends from the lower joint to the target joint, and when pressurized, it contracts. The joint has a leaf-shaped patch that provides an extra surface for bending, resulting in flexion of the inflatable joint.

In existing soft inflatable robotic arms, motors are typically placed at the base, requiring the design of rope paths inside the arm. In this study, by placing the pouch muscle between the target joint and the preceding joint to drive the system, there is no need to consider all rope paths. Instead, only one path needs to be designed for each joint, offering a significant advantage.

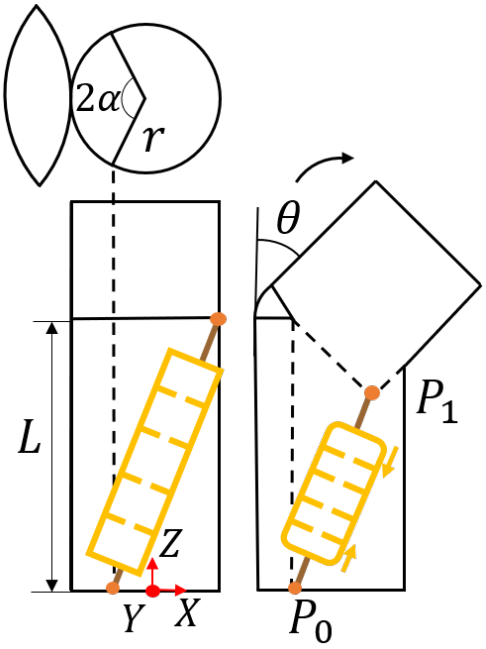

Fig. 2. Overview model for inflatable robot

B. Calculation of Pouch Muscle Length

The modeling of rope traction in the opened inflatable robot addressed in this study has been investigated in a previous study [5]. In this work, this modeling is used as a reference to calculate the length of the pouch muscle. First, as shown in Fig. 2, a coordinate system is set at the bottom of the link. The lower and upper parts of the pouch muscle are denoted as p_0 and p_1, respectively, and the design angle θ of each joint is used to calculate the required traction S. From the experimental measurements, the contraction rate of the pouch muscle was confirmed to be approximately 20 %. Therefore, the required length of the pouch muscle, P_{Length}, was calculated from the required traction using this value.

$$p_0 = [-r\cos\alpha \ 0 \ 0]^{\mathrm{T}} \tag{1}$$

$$p_1 = \begin{bmatrix} r(1+\cos\alpha)\cos\theta - r\cos\alpha \\ 0 \\ L - r(1+\cos\alpha)\sin\theta \end{bmatrix} \tag{2}$$

$$S = \|p_1 - p_0\| \tag{3}$$

$$P_{Length} = 5S \tag{4}$$

By using this calculation formula, the required length of the pouch muscle can be determined based on the design angle of each joint, the radius, the length between the links, and the parameter α that is determined during the design process.

III. DESIGN

A. Overview

A 6-degree-of-freedom robotic arm was developed, consisting of a shoulder joint, elbow joint, and a four-finger gripper that mimic human joint structures. Each of the

shoulder, elbow, and fingers has one degree of freedom, allowing smooth joint motion. The design angles and radii of each joint are listed in Table I, and the link lengths and rotation directions are shown in Fig. 3.

TABLE I
DESIGN ANGLES AND RADII PARAMETERS

Joint Position	Design Angle	Radius
Shoulder Joint	60°	75 mm
Elbow Joint	90°	50 mm
The First Joint	45°	20 mm
The Second Joint	90°	20 mm

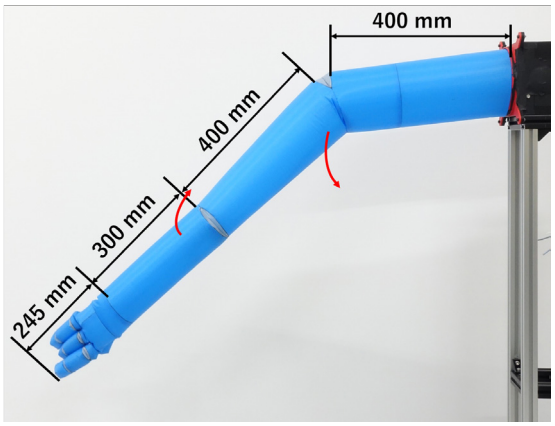

Fig. 3. Link lengths and rotation directions

For the flexion of the robotic arm, the pouch muscle is contracted, and by pulling the anchor point, the joint is bent. The extension motion is initiated by the airflow supplied by the blower.

A blower, Sanyo Denki San Ace B97 (9BMC12P2G001), was used for the air supply, and a PWM Controller from the same manufacturer was used for control. The maximum static pressure of the blower was 1950 Pa. The blower was not controlled for internal pressure but was always driven at maximum output.

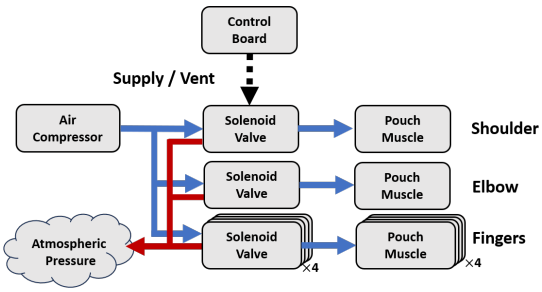

Fig. 4. A block diagram of the control system

For compressing the pouch muscles, we used a constant 14.7 kPa air pump, Yasunaga AP-80H, which supplies air to the muscles through six 3-port solenoid valves, SMC S070C-SDC-32. The solenoid valves, controlled via an Arduino, regulate the airflow into and out of each pouch muscle. Two modes are available: "Supply", in which air is delivered to contract the muscle, and "Vent", in which the structure deflates naturally as it is exposed to atmospheric pressure. The 3-port configuration allows each valve to switch between these modes, enabling precise control of the contraction and relaxation of all six pouch muscles simultaneously (Fig. 4).

The fabrication method involves sewing ripstop nylon to create the structure. The entire robotic arm needs to be flexible, lightweight, and have minimal stretching. Therefore, ripstop nylon was chosen as the material for the robotic arm, and it was sewn together using a sewing machine to construct the arm.

In this study, an inflatable gripper with one thumb and three fingers, totaling four fingers, was fabricated as a robotic gripper. The lengths of the palm and the proximal (PP), middle (MP), and distal (DP) phalanges of each finger are shown in Fig. 5.

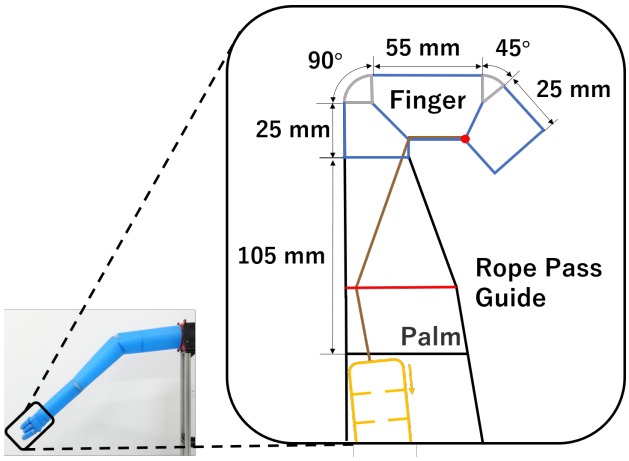

Fig. 5. Details of gripper lengths

B. Pouch Muscle Length

The calculation of the required pouch muscle length for the shoulder and elbow joints is performed. The parameters used include the target angles and radii from Table. I, the lengths of each link from Fig. 3, and $\alpha = 72°$. The required traction and pouch muscle length from the calculation results are shown in Table. II

TABLE II
REQUIRED TRACTION AND POUCH MUSCLE LENGTH

Joint Position	Required Traction Length	Pouch Length
Shoulder	92 mm	460 mm
Elbow	69 mm	345 mm
Finger	50 mm	250 mm

C. Placement of the Pouch Muscles

The position of the rope path guide and the way the pouch muscle is stretched are shown in Fig. 6.

It is necessary to fix the pouch muscle at the anchor point of the target joint and the lower joint. A guide was fabricated to determine the fixing point for the pouch muscle. The guide

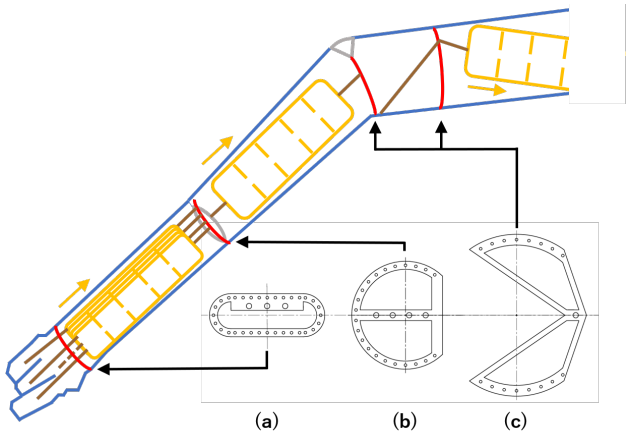

Fig. 6. Guide for fixing point of pouch muscle and rope path guide (a) Rope path guide for fingers (b) Pouch fixation guide for fingers (c) Rope path guide for shoulder joint and pouch fixation guide for elbow joint

was created to fix the pouch muscle on the opposite side of the anchor point by 180°, stretching the pouch muscle between the anchor point and the fixing point on the guide. The guide was sewn onto the seam created during the fabrication of the cylindrical structure and attached accordingly. By fabricating and sewing the guide, it became possible to place the pouch muscle between the links while ensuring the appropriate pulling angle for the target joint. Fig. 6(a) shows that the fixing point for the gripper didn't provide a sufficient pulling angle. Therefore, a rope path guide for the fingers was created to ensure the necessary pulling angle. The thumb does not have a rope path guide, but its pulling angle is maintained, and the guide functions for the other three fingers. Fig. 6(b) shows the fixing point made for the four-finger gripper. Holes were created to prevent the entanglement of pouch muscles and air tubes, allowing the attachment of each pouch muscle. The thumb is connected from the pouch fixation guide to the anchor point without passing through a rope path guide. Fig. 6(c) is used in two ways. It functions as a fixing point for the elbow joint and also serves as a rope path guide for the shoulder joint.

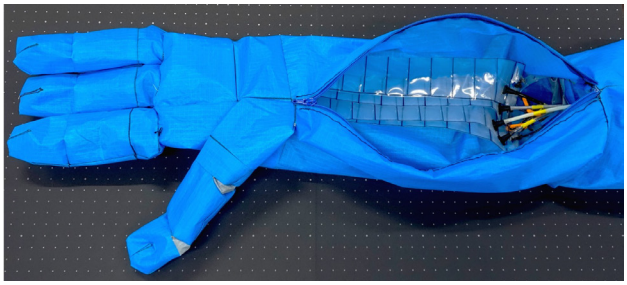

Fig. 7. The pouch muscles inside the robotic arm. Four pouch muscles are arranged inside the forearm to drive the fingers.

As shown in Fig. 7, the pouch muscles are located inside the inflatable arm. By placing the pouch muscles inside, it becomes difficult to make contact with the actuators from the outside, and even if contact occurs, the soft pneumatic actuators, which don't contain rigid components, provide a high level of safety.

IV. EXPERIMENTS

In this section, experiments were conducted to examine the effectiveness of the musculo-skin system using the developed robotic arm. First, the range of motion and bending speed of the shoulder and elbow joints were measured to evaluate the performance of joint actuation based on the musculo-skin system. Furthermore, hand gesture motions and object-grasping tasks were performed using the four-finger gripper to evaluate the fineness of motion and controllability.

A. Motion Range of the Robotic Arm

For arm evaluation, the range of motion of the shoulder and elbow joints was assessed. The evaluation method involved motion capture. The maximum angles and angle changes were output as data from the time series to assess the contraction and extension speeds. Markers were placed in the enclosed area and the angles of the markers attached to the links around the rotational joints were calculated, showing the maximum angles and data from the time series.

As shown in Fig. 8, the maximum angles were 51.2 ° for the shoulder joint and 53.7 ° for the elbow joint.

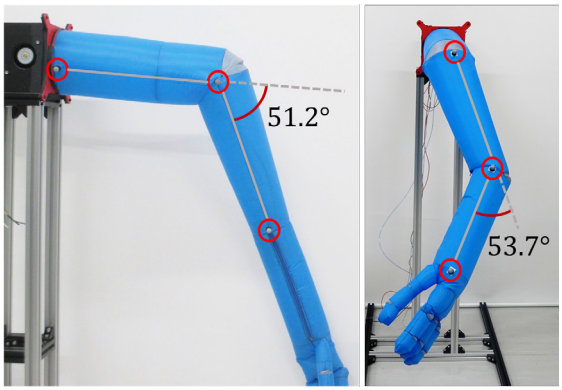

Fig. 8. Maximum rotation angles of the shoulder and elbow joints. The red-circled area in the figure is an optical marker.

A deviation of 36.3 ° from the target design angle of the elbow joint was observed when the robotic arm was placed vertically. This was likely because the arm had to move the weight of the rope path guide for finger motion, which was approximately 35 grams, against gravity. Therefore, to eliminate the influence of gravity, the robotic arm was placed horizontally, and the elbow joint angle was measured using color tracking.

As shown in Fig. 9, the maximum angle of the elbow joint was 71.4 ° when the robotic arm was placed horizontally.It was confirmed that the angle error was smaller when the robotic arm was placed horizontally and the effect of gravity was excluded, compared to when it was placed vertically. In contrast, for the shoulder joint, the error appeared to decrease due to the influence of gravity.

The calculated angles were plotted on the vertical axis, with time on the horizontal axis, and shown as data from

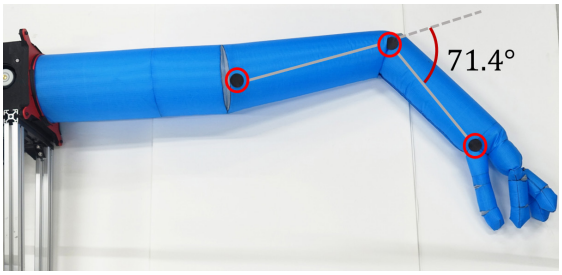

Fig. 9. Maximum rotation angle of the elbow joint when the robotic arm was positioned horizontally to exclude the effect of gravity. The red-circled area in the figure is a color marker used for tracking.

the time series. For both the shoulder and elbow joints, the pouch muscle pressurization was started simultaneously with the measurement, and the exhaust of the pouch muscle was initiated at the 30 second mark of the measurement.

The shoulder joint fully flexed in 12.3 seconds and the extension motion was completed in 26.8 seconds(Fig. 10). The elbow joint fully flexed in 6.2 seconds and the extension motion was almost completed in 7.7 seconds(Fig. 11).

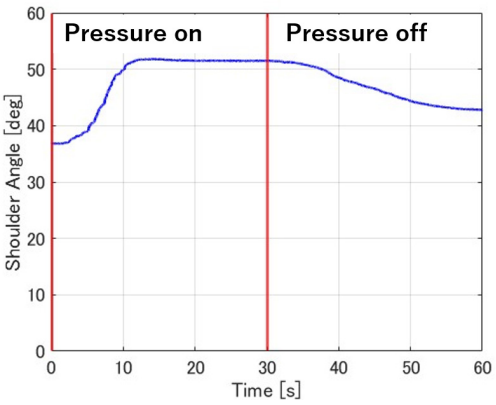

Fig. 10. Data from the time series of the shoulder joint

The difference in flexion and extension times between the shoulder and elbow joints is considered to be due to the size of the pouch muscles. Because the required air volume differs between the two joints, the time needed for air inflation and deflation is longer in the shoulder joint. In addition, since the extension motion of the shoulder joint acts against gravity, whereas the elbow joint utilizes gravity during extension, this difference is also considered to be a major factor influencing the motion time.

The reason for the longer extension time compared to the flexion time is likely that the pouch muscle is in a state of atmospheric pressure except during flexion. As a result, the air naturally escapes more slowly than during contraction. It is believed that quicker extension motion could be achieved by expelling the air from the pouch using negative pressure, but this would require an additional pump, so this study was conducted under atmospheric pressure conditions.

An error was observed in the initial position of the shoulder joint, as the initial posture was not upright but slightly

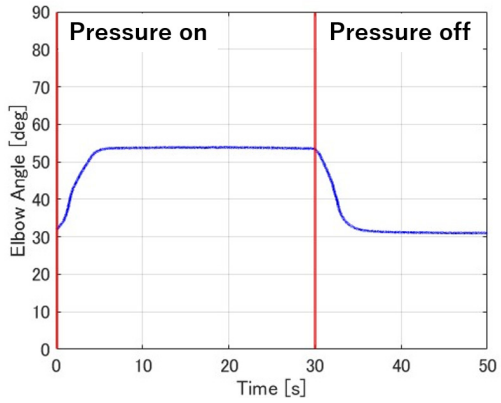

Fig. 11. Data from the time series of the elbow joint

flexed at the shoulder. This error is considered to have been caused by the distal side of the arm being heavier due to components such as the rope path guide, which prevented the arm from maintaining a fully upright position when mounted horizontally.For the error in the elbow joint, the marker was placed at the center of the robotic arm. Since the arm was designed with a tapered shape from the shoulder to the elbow, and the taper angles were different on the left and right sides, it is considered that the marker position was slightly inclined in the initial state.

B. Hand Gesture

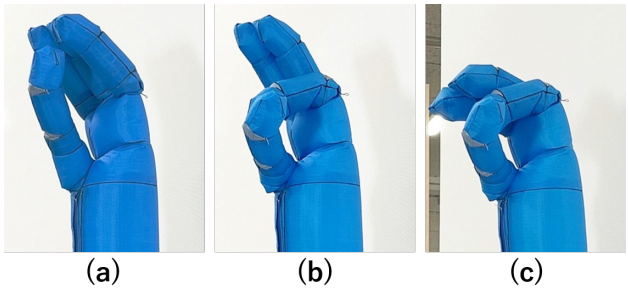

Fig. 12. Rock–Scissors–Paper gestures performed by the inflatable robotics hand: (a) Paper, (b) Scissors, and (c) Rock.

The initial position, with all fingers fully extended, was defined as the “Paper” gesture. The gesture with the thumb and third finger flexed was defined as “Scissors”, and the gesture with all fingers flexed was defined as “Rock”. Finally, the sequence returned to the “Paper” gesture. The cycle time and the duration of each gesture were measured.

As shown in Fig. 12, the sequence of movements (a)(b)(c)(a) was completed in 18 seconds from the initial open hand to returning to the same posture. The durations of each transition were 6 s from (a) to (b), 5 s from (b) to (c), and 7 s from (c) to (a). However, the posture of the open hand after the cycle differed from the initial posture.

The faster motion of the fingers compared to the shoulder and elbow joints is attributed to the use of smaller pouch

muscles in the finger joints, which enable more rapid actuation.

The discrepancy between the initial and final "Paper" gestures is believed to result from errors introduced during the sewing process. In particular, for the narrow-diameter robotic hand, such fabrication errors appear to have a significant impact on the resulting finger shapes.

C. grasping lightweight object

Fig. 13. Grasping a paper cup, holding a total weight of 14 g.

The robotic arm developed in this study is capable not only of performing gestures but also of grasping objects. As shown in Fig. 13, the arm was able to grasp an object weighing 14 g. Since it is an opened inflatable robot arm, continuously supplied with air by a blower, it cannot handle heavy objects. However, it is capable of grasping lightweight objects such as paper cups. The maximum grasping weight is 14 g, and any weight beyond this will cause the fingers to buckle, making grasping impossible.

V. CONCLUSIONS

In this study, we proposed and developed an inflatable robotic arm equipped with a novel musculo-skin system, which has six degrees of freedom including the shoulder, elbow, and fingers. To demonstrate the effectiveness and fundamental performance of the musculo-skin system, joint angles and motion speeds were measured, and gesture and object-grasping experiments were conducted to verify its functionality. As future challenges, it is necessary to reduce displacement from the initial position by improving sewing accuracy during fabrication and introducing a blower capable of supplying higher air pressure. In addition, not only the contraction amount but also the required traction force of the pouch muscle should be considered. The inflatable arm developed in this study has the potential to be applied to humanoid robots designed for human interaction, such as upper-body humanoid systems, and is expected to contribute to further research development.

ACKNOWLEDGEMENT

This work was supported by JST Moonshot R&D, Grant Number JPMJMS2013.

REFERENCES

[1] Siddharth Sanan, Michael H. Ornstein, and Christopher G. Atkeson. Physical human interaction for an inflatable manipulator. pages 7401–7404, 2011.

[2] Ronghuai Qi, Amir Khajepour, William W. Melek, Tin Lun Lam, and Yangsheng Xu. Design, kinematics, and control of a multijoint soft inflatable arm for human-safe interaction. *IEEE Transactions on Robotics*, 33:594–609, 6 2017.

[3] Ryuma Niiyama, Masahiro Ikeda, and Young Ah Seong. Inflatable humanoid cybernetic avatar for physical human–robot interaction. *International Journal of Automation Technology*, 17(3):277–283, 2023.

[4] Ryuma Niiyama, Young ah Seong, Yoshihiro Kawahara, and Yasuo Kuniyoshi. Blower-powered soft inflatable joints for physical human-robot interaction. *Frontiers in Robotics and AI*, 8, 8 2021.

[5] Katsu Uchiyama, Masayuki Otsuka, and Ryuma Niiyama. Multi-dof blower-powered and inner tendon-driven soft inflatable robotic arm. In *2024 IEEE/SICE International Symposium on System Integration (SII)*, pages 42–47, 2024.

[6] Ryosuke Tatara, Naoki Nomaguchi, Akihiro Kawamura, Ryo Kurazume, and Sadao Kawamura. Development of an inflatable robotic arm on mobile platform for fetch-and-give tasks. In *2019 IEEE/SICE International Symposium on System Integration (SII)*, pages 707–711, 2019.

[7] Namsoo Oh and Hugo Rodrigue. Toward the development of large-scale inflatable robotic arms using hot air welding. *Soft robotics*, 10:88–96, 2 2023.

[8] Charles M. Best, Joshua P. Wilson, and Marc D. Killpack. Control of a pneumatically actuated, fully inflatable, fabric-based, humanoid robot. volume 2015-December, pages 1133–1140. IEEE Computer Society, 12 2015.

[9] Siddharth Sanan, Howie Choset, Steven H Collins, and J Edward Colgate. Soft inflatable robots for safe physical human interaction. Technical report, 2013.

[10] Ryuma Niiyama, Xu Sun, Cynthia Sung, Byoungkwon An, Daniela Rus, and Sangbae Kim. Pouch motors: Printable soft actuators integrated with computational design. *Soft Robotics*, 2(2):59–70, 2015.

[11] Young Ah Seong, Ryuma Niiyama, Yoshihiro Kawahara, and Yasuo Kuniyoshi. Low-pressure soft inflatable joint driven by inner tendon. In *2019 2nd IEEE International Conference on Soft Robotics (RoboSoft)*, pages 37–42, 2019.